HEFAT2014
10th International Conference on Heat Transfer, Fluid Mechanics and Thermodynamics
14 –16 July 2014
Orlando, Florida

THERMAL AND ELECTRICAL STUDY ON AC LIGHT-EMITTING DIODE WITH QUANTUM WELLS UNDER VARIOUS COOLING RATE

Shong-Leih Lee*, Chih-Hao Cheng, Che-Hsien Ku, and Yueh Hsu
*Author for correspondence
Department of Power Mechanical Engineering,
National Tsing Hua University,
Hsinchu 30013, Taiwan,
E-mail: sllee@pme.nthu.edu.tw

ABSTRACT

The conventional Shockley equation is inappropriate to describe the relationship between the current density and the forward voltage drop across the p-n junction in LED (light-emitting diode) with multiple quantum wells. In the present study, a semi-empirical model based on the existing experimental measurements is proposed to evaluate the forwards voltage drop under given current density and temperature. The numerical model then is employed to investigate the electrical and temperature fields on ac LED with multiple quantum wells under various cooling rate. The numerical results reveal that the temperature of the LED oscillates under ac electrical potential. The temperature increases due to the heat generation arising from the electrical current across the p-n junction when the electrical potential exceeds the threshold voltage. Otherwise, there is no electrical current and thus the temperature decreases due to the effect of the cooling device. Both light-emitting power and maximum temperature increase as expected when the applied ac electrical potential increases. Fortunately, the temperature of the LED can be efficiently controlled by increasing the cooling rate. Although increasing the cooling rate would decrease the light-emitting power, the influence is not significant.

INTRODUCTION

The light-emitting diodes (LEDs) have recently been commercialized in general lighting, architecture decoration, and backlight modules. As compared to traditional light sources, LEDs have some major advantages such as longer lifetime, narrow spectrum, good mechanical stability, high color rendering index, and most importantly high energy efficiency [1-3]. However, the typical high current density occurring in high-power LEDs produces high temperature in the p-n junction of the LEDs that creates the droop effect [1, 4]. The droop effect causes great degrade in the device performance.

The relationship between the current density J and the forward voltage drop V_f across the p-n junction in a diode is known as JV curve [5, 6]. The JV curve for conventional LEDs without quantum wells is described by

$$J = J_s(\exp(\frac{eV_f}{n\,k\,(T+273)})-1) \qquad (1)$$

where J_s is the saturation current density, e is the elementary charge, k is the Boltzmann constant, and T is the temperature (in Celsius) at the p-n junction. This is the well-known Shockley equation if the ideality factor n is dropped from Eq. (1). The Shockley equation was derived by Shockley [7] under the assumption of no carrier recombination in the depletion region in 1949. Sah et al. [8] subsequently modified the equation by adding the ideality factor n to Eq. (1) with $1 < n \le 2$ to take the effect of carrier recombination into account. The modified Shockley equation is often extended to LEDs with quantum wells [9-13]. The most popular approach is to use the modified Shockley equation with a value of n that best-fits the measured JV curve.

Lee and coworkers [5, 6, 14] pointed out that the modified Shockley equation does not apply to LEDs with quantum wells for the following reasons. For LEDs without quantum wells, the current arising from the carrier recombination is significant only when the forward bias voltage is small. However, LEDs are forward-biased heavily in typical operation. Under this condition, the carrier recombination current can be entirely ignored. By contrast, for LEDs with quantum wells holes and electrons are injected into the quantum wells where one electron recombines with a hole and releases a photon. The current in LEDs with quantum wells is essentially the recombination current. The modified Shockley equation [8] formulates almost only the diffusion current, and thus cannot be used for LEDs with quantum wells.

The previous works on the modeling of the LEDs have mainly concentrated on the current transport, light extraction, optical spectrum, whereas the thermal effects, including the heat generation in the p-n junction and the heat energy extracted by the cooling device, have attained less attention. In

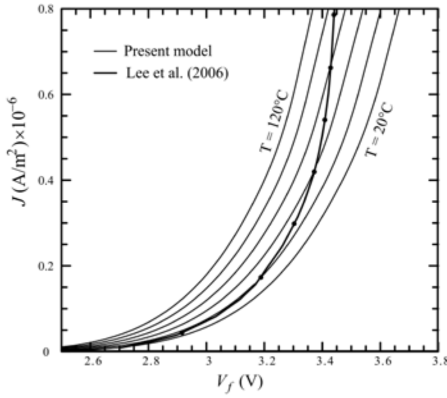

Figure 1 The proposed JV curve for the LED [6] based on the K-factor from Xi and Schubert [15].

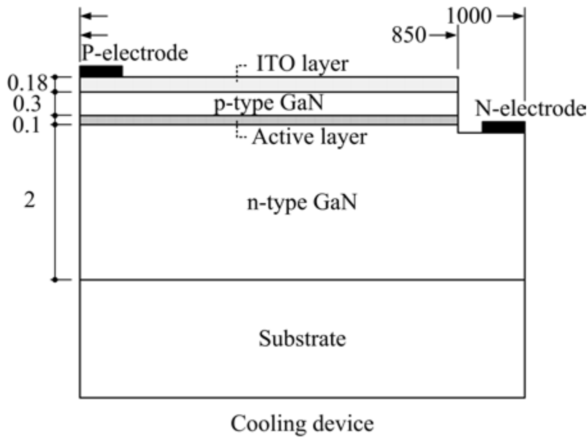

Figure 2 Geometry of the GaN-based LED under study.

the present study, a semi-empirical model based on an existing experimental measurement is demonstrated to evaluate the forwards voltage drop under given current density and temperature. The numerical model then is employed to investigate the influence of the cooling rate on ac LED with multiple quantum wells.

THORETICAL ANALYSIS

To investigate the characteristics of the JV curve for LEDs with multiple quantum wells, Lee et al. [6] fabricated a LED with multiple quantum wells, and then measured the JV curve for this particular LED. For convenience, their measured JV curve (the effect of the series resistance has been extracted) is plotted in Fig. 1. The temperature at the p-n junction of the LED estimated from the measured thermal resistance (166 K/W) between the p-n junction and the case is expressible as

$$T = 166 J V_f + 27 \tag{2}$$

where T is in Celsius. The seven black dots on the JV curve in Fig. 1 denote the temperature at $T = 30°C$, $40°C$, …, $90°C$ according to Eq. (2). Due to the lack of more reliable experimental data, the derivative of the junction voltage with respect to the junction temperature (known as K-factor) for a GaN ultraviolet LED

$$\frac{\partial V_f(T,J)}{\partial T} = -0.0023 \text{ V/K} \tag{3}$$

from Xi and Schubert [15] is assumed valid for the present LED with multiple quantum wells. This leads to a system of temperature dependent JV curves as shown in Fig. 1.

On introducing the dimensionless transformation

$$\xi = 25\left(\frac{V_f}{V_{f0}} - 1\right), \quad j = \frac{J}{J_0} \tag{4}$$

the JV curves in Fig. 1 essentially merge into a single function (Bernoulli function) in the low current density limit

$$j = B(\xi) = \frac{\xi}{1 - \exp(-\xi)} \tag{5}$$

while become linear functions in the high current density limit

$$j = a\xi \tag{6}$$

where

$$V_{f0} = 3.443 + (13.2T^2 - 4440T) \times 10^{-6} \ V$$

$$J_0 = 10.53T^2 - 1458T + 296600 \ A/m^2 \tag{7}$$

$$a = (3.983T^2 - 406.3T + 111200)\frac{V_{f0}}{J_0} \tag{8}$$

In the formulation, a is dimensionless while T is in Celsius. To achieve a smooth transition between the Bernoulli function (5) and the linear function (6), the JV curve at a constant temperature is approximated with a Hermite polynomial by letting ξ be a cubic polynomial of j in the interval $\gamma_1 \le j \le \gamma_2$, where $\gamma_1 = j_b - 0.48$, $\gamma_2 = j_b + 0.48$, $j_b = a\xi_0$ with $\xi_0 = \ln(\frac{a}{a-1})$ being the intersection of the Bernoulli function (5) and the linear function (6).

Figure 2 shows a schematic diagram of typical LEDs with multiple quantum wells. The LED analyzed in the present study is a square chip of dimension $L = 1000 \ \mu m$. The multiple quantum wells are located inside the active layer. The electrical and thermal conductivities for the n-GaN, p-GaN, and ITO from the literature and that employed in the present study are $\sigma_{ITO} = 400$, $\sigma_p = 0.02$, $\sigma_n = 20$ (unit $10^3 S/m$), and $k_n = 120 W/mK$. Use of the ITO layer is to achieve a good current spreading. It is important to note that the electrical conductivity of the p-GaN layer is very small as compared to that of the n-GaN layer and the ITO layer. Moreover, there is a great electrical potential drop across the active layer. Hence, the electrical current would spread along the ITO layer, and then goes through the p-GaN layer and active layer normally (vertically) on its way to the n-GaN layer [16], if an electrical potential is applied on the p-electrode while the n-electrode is grounded. This implies that the p-GaN layer and active layer can be treated as a contact resistance between the ITO and the n-GaN layer.

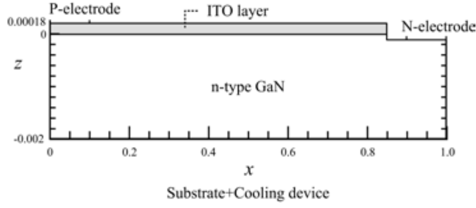

Figure 3 The simplified problem configuration for the LED under study.

Based on the characteristics of the LEDs, the problem configuration is simplified as that revealed in Fig. 3 where the p-GaN layer and active layer are represented by the plane of $z = 0$. Let an ac electrical potential of frequency f and amplitude V_0 be applied on the p-electrode, while the n-electrode is grounded. The electrical field is insulated on all of the boundaries except for the electrodes. In the thermal field, one assumes that 25% of the energy consumption in the active layer (conversion efficiency $\eta_{ce} = 0.25$) transfers to the environment by light-emitting through the p-GaN layer and ITO layer [17, 18]. The other 75% of the energy (including the heat generated by light absorption inside the LED chip) as well as the joule heating is extracted with the cooling device. Effect of natural convection on all of the boundaries is neglected.

Figure 4 illustrates a commercial ac LED bulb with fin cooling device. The electrical circuit is precisely designed such that each LED receives only forward electrical current. All of the LED chips share the same cooling device. The overall heat transfer coefficient over the substrate and the cooling device is defined by

$$U = \frac{\overline{q}}{(\overline{T} - T_\infty)} \frac{A_{fin}}{A}$$

$$\overline{q} = \frac{1}{A_{fin}} \int_{A_{fin}} h_e \, (T_{fin} - T_\infty) \, ds \tag{9}$$

where $\overline{q}$ represents the mean heat flux on the fin surface, $\overline{T}$ is the mean temperature on the bottom surface of the n-GaN layer, h_e is heat transfer coefficient on the fin surface, T_{fin} is the fin surface temperature, and T_∞ is the ambient temperature. The fin surface area is far greater than that of the n-GaN layer ($A_{fin} >> A$). The typical overall heat transfer coefficient U is in the range of $200 - 1000 W/m^2K$. Some particular design in laboratory was reported to reach 40,000 W/m^2K [19]. Due to the temperature dependence of the JV curve, the heat transfer in LEDs is a thermal-electrical coupling problem.

After making the dimensionless transformation

$$x = \frac{X}{L}, \; z = \frac{Z}{L}, \; \hat{\sigma} = \frac{\sigma}{\sigma_{ITO}}, \; \phi = \frac{V}{V_0}, \; j_z = \frac{J\,L}{\sigma_{ITO} V_0}$$

$$\theta = \frac{T - T_\infty}{T_c}, \; T_c = \frac{\sigma_n V_0}{k_n}, \; \hat{t} = \frac{\alpha_n t}{L^2}, \; \alpha_n = \frac{k_n}{\rho_n (c_p)_n}$$

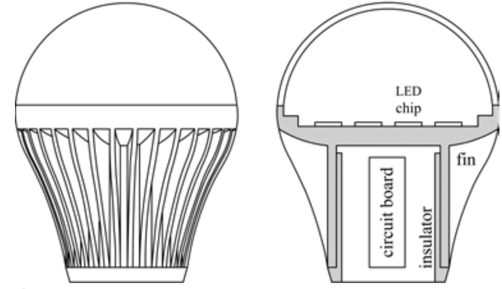

Figure 4 A schematic diagram of a commercial ac LED bulb with fin cooling device.

$$Bi = \frac{U\,L}{k_n}, \; \Omega = \frac{2\pi\, f\, L^2}{\alpha_n}, \; \beta_n = \frac{\sigma_n}{\sigma_{ITO}}, \; \beta_p = \frac{\sigma_p}{\sigma_{ITO}} \tag{10}$$

the electrical and energy equations are, respectively,

$$\frac{\partial}{\partial x}(\hat{\sigma}\frac{\partial \phi}{\partial x}) + \frac{\partial}{\partial z}(\hat{\sigma}\frac{\partial \phi}{\partial z}) = 0 \tag{11}$$

$$\frac{\partial \theta}{\partial \hat{t}} = \frac{\partial^2 \theta}{\partial x^2} + \frac{\partial^2 \theta}{\partial z^2} + (\frac{\partial \phi}{\partial x})^2 + (\frac{\partial \phi}{\partial z})^2 \tag{12}$$

where the source term in the RHS of Eq. (12) is the joule heating. The electrical conductivity $\hat{\sigma}$ is a step function. It has the value of unity in the ITO layer and jumps to β_n in the n-GaN layer. The "contact resistance" between the ITO layer and the n-GaN layer is

$$\Re_c = \frac{h_p}{\beta_p} + \frac{\phi_f}{j_z} \quad \text{at } 0 \le x \le 0.85 \text{ and } z = 0 \tag{13}$$

where h_p is the thickness of the p-GaN layer, $j_z = \partial \phi / \partial z$ is the dimensionless downward vertical current density on the ITO side of the "interface" and $\phi_f = V_f / V_0$ is the forward voltage drop across the p-n junction. The associated boundary conditions on the electrodes are

$$\phi = \sin(\Omega \hat{t}) \quad \text{at } 0 \le x \le 0.1 \text{ and } z = 0.00018$$

$$\phi = 0 \quad \text{at } 0.9 \le x \le 1 \text{ and } z = -0.00010 \tag{14}$$

For direct current, the function $\sin(\Omega \hat{t})$ should be replaced by unity. Other boundaries are insulated as mentioned earlier. For thermal analysis, one needs to solve only the heat transfer inside the n-GaN layer, since the ITO layer is a thin and good electrical conductor. Moreover, the natural convection above the LED is negligible. In this connection, the heat generation in the p-GaN layer as well as the active layer is treated as a surface heat flux for simplicity. Hence, the associated boundary conditions for the energy equation (12) are expressible as

$$\frac{\partial \theta}{\partial z} = j_z (\frac{h_p}{\beta_p} j_z + (1 - \eta_{ce})\phi_f) \quad \text{at } 0 \le x \le 0.85 \text{ and } z = 0 \tag{15a}$$

$$\frac{\partial \theta}{\partial z} - Bi\,\theta = 0 \quad \text{at } 0 \le x \le 1 \text{ and } z = -0.00200 \tag{15b}$$

All of other boundary conditions are insulated.

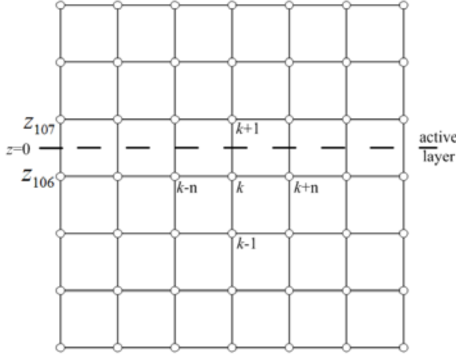

Figure 5 The grid system employed in the computation.

NUMERICAL METHOD

The thermal-electrical problem is solved on a uniform rectangular grid system with the grid mesh

$$x_i = (i-1)\Delta x\,,\quad z_l = (l-106.5)\Delta z \tag{16}$$

where $\Delta x = 0.01$, $i = 1, 2, ..., m$, $m = 101$, and $\Delta z = 0.00001895$, $l = 1, 2, ..., n$, $n = 116$. After discretized with the central difference scheme, the electrical equation (11) becomes

$$(a_W)_k \phi_{k-n} + (a_S)_k \phi_{k-1} + (a_P)_k \phi_k + (a_N)_k \phi_{k+1} + (a_E)_k \phi_{k+n} = (a_R)_k \tag{17a}$$

$$(a_W)_k = \frac{\hat{\sigma}}{(\Delta x)^2}\,,\quad (a_E)_k = \frac{\hat{\sigma}}{(\Delta x)^2}\,,\quad (a_S)_k = \frac{\hat{\sigma}}{(\Delta z)^2}\,,$$

$$(a_N)_k = \frac{\hat{\sigma}}{(\Delta z)^2}$$

$$(a_P)_k = -(a_W)_k - (a_E)_k - (a_S)_k - (a_N)_k\,,\quad (a_R)_k = 0 \tag{17b}$$

where ϕ_k represents the electrical potential at the grid point (x_i, z_l). It is the k-th grid point if the grid points are numbered with $k = (i-1)n + l$ [20]. The active layer ($z = 0$) is located in between z_{106} and z_{107}, and thus the conductivity $\hat{\sigma}$ is unity for $l \geq 107$, and β_n for $l \leq 106$. The electrical resistance (*ER*) between $l = 106$ and $l = 107$ is

$$ER = \frac{\Delta z}{2\beta_n} + \Re_c + \frac{\Delta z}{2} \tag{18}$$

This gives rise to the weighting factors

$$(a_N)_k = (a_S)_{k+1} = \frac{\hat{\sigma}_{ex}}{(\Delta z)^2} \tag{19}$$

$$\hat{\sigma}_{ex} = \left(\frac{1}{2\beta_n} + \frac{\Re_c}{\Delta z} + \frac{1}{2}\right)^{-1} \tag{20}$$

at $k = (i-1)n + 106$ (see Fig. 5). The notation $\hat{\sigma}_{ex}$ will be referred to as the extended electrical conductivity in the present work. Similarly, the discretized energy equation (12) can be written as

$$(b_W)_k \theta_{k-n} + (b_S)_k \theta_{k-1} + (b_P)_k \theta_k + (b_N)_k \theta_{k+1} + (b_E)_k \theta_{k+n} = (b_R)_k \tag{21a}$$

$$(b_W)_k = \frac{1}{(\Delta x)^2}\,,\quad (b_E)_k = \frac{1}{(\Delta x)^2}\,,\quad (b_S)_k = \frac{1}{(\Delta z)^2}\,,$$

$$(a_N)_k = \frac{1}{(\Delta z)^2}$$

$$(b_P)_k = -(b_W)_k - (b_E)_k - (b_S)_k - (b_N)_k - \frac{1}{\Delta \hat{t}}$$

$$(b_R)_k = -\left(\frac{\phi_{k+n} - \phi_{k-n}}{2\Delta x}\right)^2 - \left(\frac{\phi_{k+1} - \phi_{k-1}}{2\Delta z}\right)^2 - \frac{\theta_0}{\Delta \hat{t}} \tag{21b}$$

In the discretization procedure, the unsteady term has been discretized with the implicit scheme, i.e.

$$\frac{\partial \theta}{\partial \hat{t}} = \frac{\theta - \theta_0}{\Delta \hat{t}} \tag{22}$$

where θ_0 stands for the temperature at the previous time step $\hat{t}_0 = \hat{t} - \Delta \hat{t}$. As mentioned earlier, one solves only the n-GaN layer for the temperature. The active layer along with the p-GaN layer is treated as a Neumann boundary condition (15a) at $z = 0$.

For convenience, the numerical algorithm is described as follows.

(1) Set the initial temperature θ_0 for the initial time $\hat{t}_0 = 0$.
(2) Guess the electrical potential ϕ and the temperature θ for the present time $\hat{t} = \hat{t}_0 + \Delta \hat{t}$.
(3) Compute $j_z = \partial \phi / \partial z$ on the ITO side.
(4) Determine ϕ_f from the JV curve revealed in Fig. 1.
(5) Evaluate $\hat{\sigma}_{ex}$ from Eqs. (13) and (20).
(6) Renew the electrical potential ϕ by solving the matrix equation constituted by Eqs. (17), (19) and the associated boundary conditions.
(7) Renew the temperature θ by solving Eq. (12) with the boundary condition (15) and the other insulation boundary conditions.
(8) Return to Step 3 and repeat the computations until both ϕ and θ converges within a prescribed tolerance.
(9) Stop computation if the prescribed time limit is reached. Otherwise, set the "previous" temperature by letting $\theta_0 = \theta$, and then go back to Step 3 for the next time step.

In Step 4, the forward voltage drop V_f across the p-n junction according to the current density

$$J = \frac{\sigma_{ITO} V_0}{L} j_z \tag{23}$$

is determined by the JV curve of the LED under given temperature. During the loop of Steps 3-8, successive-over-relaxation factors (SOR_ϕ for the electrical potential in Step 6 and SOR_θ for the temperature in Step 7) might be needed. The value of $SOR_\phi = SOR_\theta = 1$ with a tolerance of 5×10^{-6} is employed in the present study. To gain a good numerical stability, the finite difference equation (21) is solved with the SIS solver [20].

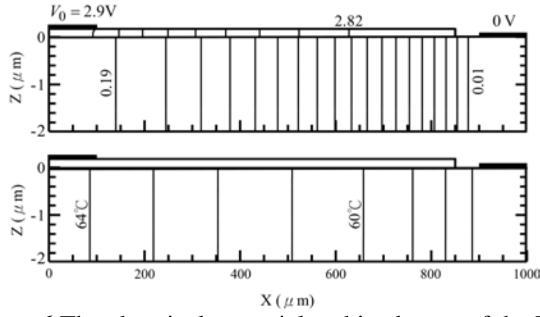

Figure 6 The electrical potential and isotherms of the LED under direct current.

RESULTS AND DISCUSSION

The characteristics of LED depend strongly on the material and structure of the diode. In this section the LED fabricated by Lee et al. [6] is investigated for a better understanding on LEDs with multiple quantum wells. All of the test cases are based on the ambient temperatures of $T_\infty = 26°C$. The frequency of the alternating current applied on the p-electrode is $f = 60Hz$. Figure 6 shows the resulting electrical potential and isotherms when a dc electrical potential $V_0 = 2.9V$ is applied on the p-electrode. The overall heat transfer coefficient of the cooling device is $U = 1000W/m^2K$. It is important to see that the electrical current spreads through the ITO layer with only minor voltage drop (from 2.90V to 2.81V). Similarly, the electrical potential in the n-GaN layer decreases from 0.20V to zero. The major voltage drop seems to occur in the active layer and p-GaN layer. The temperature in the n-GaN layer is found to be in the range of $57-64.5°C$. The maximum temperature occurs at the point $(X, Z) = (0,0)$.

Figure 7 reveals the maximum temperature for an alternating current of amplitude $V_0 = 3.3V$ under two representative overall heat transfer coefficients, i.e. $U = 200W/m^2K$ and $1000W/m^2K$. The maximum temperature is seen to oscillate at frequency $f = 60Hz$ when the alternating current is applied on the p-electrode. For $U = 200W/m^2K$, the maximum temperature reaches the dynamic "steady-state" approximately 0.2 s after the electrical power is turned on. It takes less time for a larger cooling rate (e.g. 0.02 s for $U = 1000W/m^2K$). For the case of $V_0 = 3.3V$ and $U = 1000W/m^2K$, the light-output power

$$P = (\sigma_{ITO} V_0^2 L)\, \eta_{diod} \int_{0.10}^{0.85} j_z \phi_f \, dx \tag{24}$$

generated in the p-n junction under dynamic steady-state is shown in Fig. 8 for a period of oscillation ($0 \le t^* \le 0.01667\, s$ with t^* being the time counting from the beginning of each period). Note that the light-emitting in the region beneath the p-electrode ($0 \le x < 0.10$) has been excluded from the integration (24) because the electrode is opaque. The dashed lines in Fig. 8 denote the times when the alternating current reaches the voltage peaks. The corresponding maximum temperature variation is also provided in Fig. 8. As expected, light emits only in the time interval $0.002154\, s \le t^* \le 0.006419\, s$ when the forward voltage drop exceeds the threshold value. The maximum temperature increases rapidly during this particular time interval, and gradually decreases thereafter. It is interesting to note that there is a time lag of $0.3125 \times 10^{-3} s$ between the peaks of the light-emitting power and the alternating current due to the temperature dependence of the JV curve. The forward voltage drop V_f will decrease when the temperature increases (see Fig. 1). This gives rise to a sharply increasing current density and

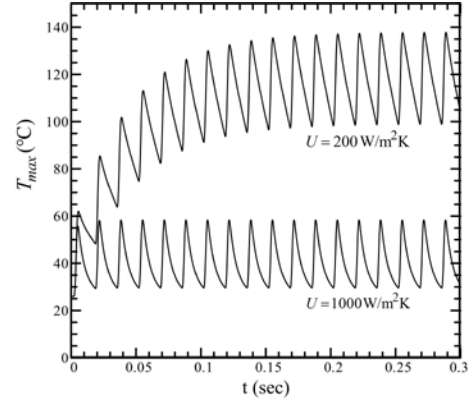

Figure 7 Variation of the maximum temperature for $V_0 = 3.3V$ under two representative overall heat transfer coefficients.

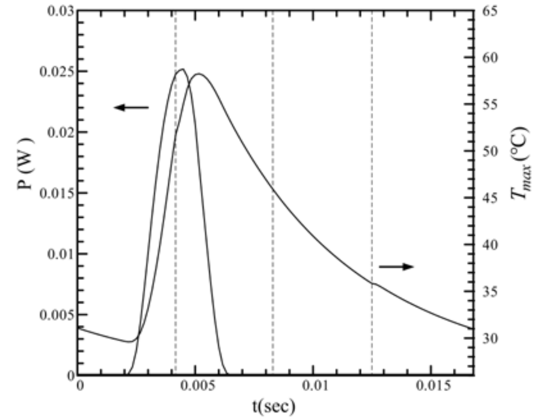

Figure 8 The light-output power in the quasi-static state for a period of oscillation under $V_0 = 3.3V$ and $U = 1000W/m^2K$.

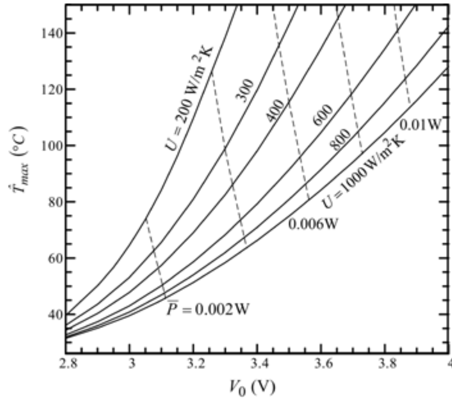

Figure 9 The value of $\hat{T}_{\max}$ as a function of V_0 under various cooling rate.

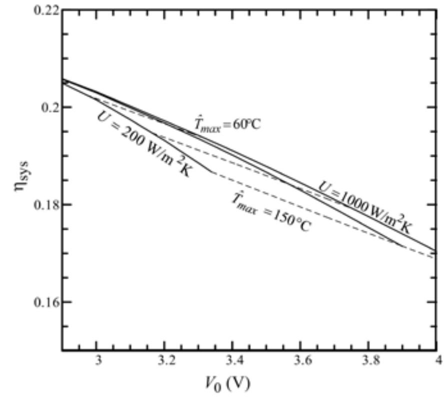

Figure 12 The system efficiency η_{sys} as a function of V_0 under various cooling rates.

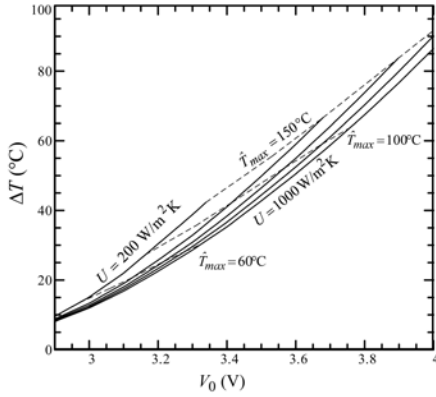

Figure 10 The peak-to-peak amplitude of the maximum temperature ΔT as a function of V_0 under various cooling rates.

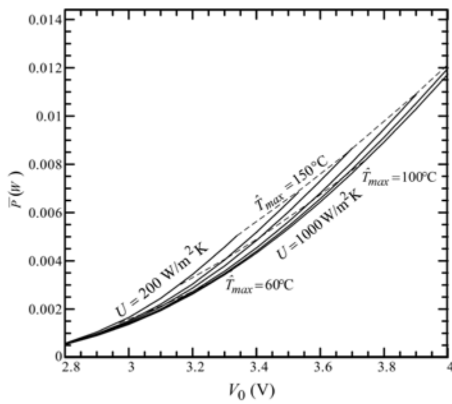

Figure 11 The average light-emitting power $\overline{P}$ as a function of V_0 under various cooling rates.

thus an increasing light-emitting power (24), if the total voltage drop between the electrodes maintains constant.

As illustrated in Figs. 7 and 8, the maximum temperature oscillates all the time when the alternating current is turned on. For convenience, the maximum value and the peak-to-peak amplitude of the maximum temperature are denoted by $\hat{T}_{\max}$ and ΔT , respectively. Both $\hat{T}_{\max}$ and ΔT possess constant value at dynamic steady-state. Figure 9 shows the value of $\hat{T}_{\max}$ as a function of V_0 under various cooling rate. The dashed curves represent the average light-output power over the whole time period at dynamic steady-state

$$\overline{P} = f \int_0^{1/f} P \, dt^* \tag{25}$$

It is evidenced from Fig. 9 that the maximum temperature can be efficiently controlled by the cooling rate. For instance, $\hat{T}_{\max}$ decreases from $138°C$ to $62°C$ at $V_0 = 3.3V$ when the overall heat transfer coefficient increases from 200 to $800\, W/m^2K$ at essentially the same light-emitting power.

Figures 10-12 show, respectively, the peak-to-peak amplitude of the maximum temperature ΔT , the average light-emitting power $\overline{P}$, and the system efficiency η_{sys} as functions of V_0 under various cooling rates. The dashed curves denote three representative maximum temperatures ($\hat{T}_{\max}$) of $60°C$, $100°C$, and $150°C$. The energy consumption and its mean value over an oscillation period are, respectively,

$$E = (\sigma_{ITO} V_0^2 L) \sin(2\pi f t^*) \int_0^{0.85} j_z \, dx$$

$$\overline{E} = f \int_0^{1/f} E \, dt^* \tag{26}$$

The system efficiency η_{sys} is defined by the ratio of $\overline{P}$ and $\overline{E}$. The numerical results reveal that increasing the cooling rate

increases the system efficiency η_{sys} and decreases both maximum value $\hat{T}_{\max}$ and peak-to-peak amplitude ΔT of the maximum temperature. It seems very good for the LEDs by increasing the cooling rate, although the light-emitting power might be slightly decreased (see Fig. 11).

Finally, it is mentioned that the JV curve for LEDs with multiple quantum wells vary from one LED to another depending on the material and structure of the LED that the conventional Shockley equation cannot predict. Unfortunately, no simple algebraic function is available to predict the JV curve for all of LEDs with multiple quantum wells so far. The present study illustrates a simple numerical method for the LED fabricated by Lee et al. [6] successfully. This numerical technique is believed to apply to most LEDs as well. Note also that a slight change in the forward voltage drop V_f during the solution procedure might cause a great deal of variation for the current density according to the JV curve (see Fig. 1). To achieve a good numerical stability, the forward voltage drop V_f is determined from a given current density in the numerical algorithm Step 4, and thus a shooting method is needed when $j < \gamma_1$ owing to the nonlinear Bernoulli function (5).

CONCLUSION

In the present study, a semi-empirical model based on the existing experimental measurements is proposed to evaluate the forwards voltage drop under given current density and temperature. The numerical model then is employed to investigate the electrical and temperature fields on ac LED with multiple quantum wells under various cooling rate. Based on the numerical results, the following conclusions are dawn.

1. The temperature of the LED oscillates under ac electrical potential. The temperature increases due to the heat generation arising from the electrical current across the p-n junction when the electrical potential exceeds the threshold voltage. Otherwise, there is no electrical current and thus the temperature decreases due to the effect of the cooling device.
2. Both light-emitting power and maximum temperature increase when the applied ac electrical potential increases.
3. The temperature of the LED can be efficiently controlled by increasing the cooling rate. Although increasing the cooling rate would decrease the light-emitting power, the influence is not significant.

REFERENCES

[1] Li, C.K., and Wu, Y.R., Study on the current spreading effect and light extraction enhancement of vertical GaN/InGaN LEDs, *IEEE Trans. on Electron Devices*, Vol. 59, 2012, pp. 400-407

[2] Hwu, F.S., Chen, J.C., Tu, S.H., Sheu, G.J., Chen, H.I., and Sheu, J.K., A numerical study of thermal and electrical effects in a vertical LED chip, *Journal of Electrochemical Society*, Vol. 157, 2010, pp. H31-H37

[3] Heikkila, O., Oksanen, J., and Tulikki, J., The challenge of unity wall plug efficiency: the effects of internal heating on the efficiency of light emitting diodes, *Journal of Applied Physics*, Vol. 107, 2010, 033705

[4] Kudryk, Y.Y., and Zinovchuk, A.V., Efficiency droop in InGaN/GaN multiple quantum well light-emitting diodes with nonuniform current spreading, *Semicon. Sci. Technol.*, Vol. 26, 2011, 095007

[5] Park, J, and Lee, C.C., An electrical model with junction temperature for light-emitting diodes and the impact on conversion efficiency, *IEEE Electron Device letters*, Vol. 26, 2005, pp. 308-310.

[6] Lee, C.C., Chen W.V., and Park, J., A new I-V model for light-emitting devices with quantum well, *Microelectronics Journal*, Vol. 37, 2006, pp. 1335-1338

[7] Shockley, W., The theory of p-n junctions in semiconductors and p-n junction transistors, *Bell Syst. Tech. Journal*, Vol. 8, 1949, p. 435

[8] Sah C.T., Noyce, R.N., and Shockley, W., Carrier generation and recombination in p-n junction and p-n junction characteristics, Pro. IRE 45, 1957, p. 1228

[9] Casey Jr, H.C., and Panish, M.B., Heterostructure lasers part A: fundamental principles, Academic Press, New York, 1978.

[10] Chitnis, A., Kumar, A., Shatalov, M., Adivarahan, V., Lunev, A., Yang, J.W., Simin, G., Asif Khan, Gaska, R., and Shur, M., High-quality p-n junctions with quaternary AlInGaN/InGaN quantum wells, *Applied Physics Letters*, Vol. 77, 2000, pp. 3800-3802

[11] Cao X.A., Stokes, E.B, and Sandvik, P.M., Diffusion and tunneling currents in GaN/INGaN multiple quantum well light-emitting diodes, *IEEE Electron Device letters*, Vol. 23, 2002, pp. 535-537

[12] Kim, H., Park, S., and Hwang, H., Design and fabrication of high efficient GaN based light emitting diodes, *IEEE Trans. on Electron Devices*, Vol. 49, 2002, pp. 1715-1722

[13] Shah, J.M., Lee Y.L., Gessmann, Th., and Schubert, E.F., Experimental analysis and theoretical model for anomalously high ideality factors (n>>2.0) in AlGaN/GaN p-n junction diodes, *Journal of Applied Physics*, Vol. 94, 2003, pp. 2627-2630

[14] Lee C.C., and Park, J., Temperature measurement of visual light-emitting diodes using nematic liquid crystal thermography with laser illumination, *IEEE Photon. Tech. Letter*, Vol. 16, 2004, pp. 1706-1708

[15] Xi, Y., and Schubert, E.F., Junction-temperature measurement in GaN ultraviolet light-emitting diodes using diode forward voltage, *Applied Physics letters*, Vol. 85, 2004, pp. 2163-2165

[16] Sheu, G.J., Hwu, F.S., Chen, J.C., Sheu, J.K., Tu, S.H., and Lai, W.C., Effect of electrode pattern on current spreading and driving voltage in a GaN/Sapphire LED chip, *Journal of Electrochemical Society*, Vol. 155, 2008, pp. H836-H840

[17] Lee, Y.J., Lee, C.J., and Chen C.H., Estimating the junction temperature of InGaN and AlGaInP light-emitting diode, Japanese Journal of Applied Physics, Vol 50, 2011, 04DG18

[18] Hwu, F.S., Sung, T.H., Chen C.H., Tseng J.W., Qiu, H., and Chen, J.C., A numerical model for studying multimicrochip and single-chip LEDs with an interdigitated mesa geometry, IEEE Photonics Journal, Vol. 5, 2013, 6600515

[19] Hwu, F.S., and Hsieh, H.L., Numerical study of thermal behavior in alternating current light-emitting diode, Advances in Mechanical Engineering, Vol. 2013, 2013, 426767

[20] Lee, S.L., A strongly-implicit solver for two-dimensional elliptic differential equations, *Numer. Heat Transfer* B, Vol. 16, 1989, pp. 161-178